

Young's Modulus Reconstruction for Elasticity Imaging of Deep Venous Thrombosis: Animal studies

S. R. Aglyamov^{a,e}, H. Xie^b, K. Kim^b, J. M. Rubin^c, M. O'Donnell^b,
T.W. Wakefield^d, D. Myers^d, and S.Y. Emelianov^a

^aDepartment of Biomedical Engineering, University of Texas at Austin, Austin TX 78759, USA;

^bDepartment of Biomedical Engineering, University of Michigan, Ann Arbor, MI 48109, USA;

^cDepartment of Radiology, University of Michigan, Ann Arbor, MI 48109, USA;

^dDepartment of Surgery, University of Michigan, Ann Arbor, MI 48109, USA;

^eInstitute of Mathematical Problems in Biology, Russian Acad. Sci., Pushchino 142290 Russia

ABSTRACT

Recently, it was suggested that ultrasound elasticity imaging can be used to age deep vein thrombosis (DVT) since blood clot hardness changes with fibrin content. The main components of ultrasound elasticity imaging are deformation of the object, speckle or internal boundary tracking and evaluation of tissue motion, measurement of strain tensor components, and reconstruction of the spatial distribution of elastic modulus using strain images.

In this paper, we investigate a technique for Young's modulus reconstruction to quantify ultrasound elasticity imaging of DVT. *In-vivo* strain imaging experiments were performed using Sprague-Dawley rats with surgically induced clots in the inferior vena cava (IVC). In this model, the clot matures from acute to chronic in less than 10 days. Therefore, nearly every 24 hours the strain imaging experiments were performed to reveal temporal transformation of the clot. The measured displacement and strain images were then converted into maps of elasticity using model-based elasticity reconstruction where the blood clot within an occluded vein was approximated as a layered elastic cylinder surrounded by incompressible tissue. Results of this study demonstrate that Young's modulus gradually increases with clot maturity and can be used to differentiate clots providing a desperately needed clinical tool of DVT staging.

Keywords: DVT, Elasticity imaging, Speckle tracking, Young's modulus, Ultrasound, Elasticity reconstruction

1. INTRODUCTION

Deep venous thrombosis (DVT) is a significant clinical problem. Pulmonary embolism is one of the complications of DVT representing the leading cause of preventable in-hospital mortality in the USA and other developed countries¹. In pulmonary embolism, the portion of blood clot detaches from the vessel wall and travels through the veins into the lung, where it can lodge in a pulmonary artery. The level of pulmonary embolism risk and DVT treatment depend on the age of the clot. Therefore it is clinically important to distinguish between acute and chronic DVT. A patient with acute DVT is treated with heparin followed by oral anticoagulants, whereas one with chronic DVT is treated with oral anticoagulants alone because the stronger anticoagulant and anti-inflammatory effects of heparin are not required². Further, one would like to avoid the use of heparin if at all possible. Heparin is a powerful anticoagulant that must be injected, and it has a higher risk of bleeding than oral anticoagulants. In fact, studies have shown that the risk of bleeding with heparin is 11% during the first 5 to 10 days of therapy³.

Although presence of DVT can be detected with objective tests, where the most common test is duplex ultrasound that combines gray-scale, color-flow Doppler, and compression ultrasound⁴, now there are no good noninvasive methods to determine clot age. The preliminary results from our previous studies suggest that ultrasound elasticity

imaging can be used to determinate the maturity of DVT⁵⁻⁹. This is based on the assumption that the Young's modulus of clots monotonically changes with fibrin and collagen concentration. Since the fibrin and collagen content of a clot increases over time, thrombus hardens with its organization. Consequently, if the elastic properties of clot can be estimated remotely, elasticity imaging can become an important clinical tool to age DVT.

Ultrasound elasticity imaging aims to assess non-invasively the elastic properties of soft tissues. One of the approaches in elasticity imaging is based on external mechanic deformation of the object and measurement of the response - internal tissue motion - with ultrasound using some kind of speckle tracking algorithm. Using inverse problem formulations, the elasticity (Young's modulus) distribution is evaluated using the distribution of the strain tensor components computed based on measured displacement vector fields. Initially elasticity imaging was developed for noninvasive diagnosis of cancer in soft tissue, but then the approach proved to be useful in various other applications¹⁰⁻¹¹.

We have proposed a "triplex" ultrasound imaging method combining conventional duplex ultrasound with elasticity imaging to detect, diagnose, and stage DVT⁶. To make triplex ultrasound a routine clinical procedure, elasticity information most probably will be acquired during free-hand scanning and compression. To test for a blood clot in the femoral vein, for example, compression ultrasound is performed by marching down a subject's leg, imaging the femoral vein in transverse orientation while simultaneously deforming the vein with the scanhead⁶. If a venous thrombus is not present, the walls of the vein quickly coapt before the adjacent artery collapses. If a thrombus is present, the arterial walls coapt before the vein's⁴. Since the compression ultrasound technique already has all the initial ingredients of elasticity imaging (i.e., external deformation of the object during continuous ultrasound imaging), it is possible to develop DVT elasticity imaging as a simple adjunct to the existing procedure.

In addition, elasticity imaging has several other important advantages as a DVT staging tool. For example, deformations that are required in compression ultrasound are binary - either the vein or artery needs to collapse for DVT detection. In elasticity imaging, a smaller degree of compression is required for DVT diagnosis since deformations within and outside of the vein are measured and analyzed. Therefore, smaller compressions are theoretically possible in DVT elasticity imaging compared to duplex ultrasound. Furthermore, the quantitative reconstruction of DVT elasticity can be eased based on geometry of the vein and clot. Indeed, the cylindrical shape of the vessel permits the use of a relatively simple mathematical model to reconstruct elastic properties of the clot where the parameters of the model such as the overall geometry of the clot are well identified from the 2D ultrasound gray-scale images.

In the model-based elasticity reconstruction method, the analytical solution to the forward elastic problem for an arbitrary planar deformation is derived first. The solution of the forward elastic problem is then used to reconstruct the unknown elasticity distribution in a region of interest (ROI) based on the iterative comparison and error minimization between ultrasonically measured and theoretically predicted deformations. The Young's modulus distribution that provides the best agreement is assumed to describe the distribution of elastic properties of the clot, vessel wall and surrounding tissue. In our previous study⁹ the proposed approach was tested using numerical simulations, experiments with tissue-equivalent phantoms, and in-vivo animal studies of stasis induced DVT. Results of reconstructed elasticity distributions clearly show that the model is appropriate for aging DVT.

In this paper, we further test model-based Young's modulus reconstruction using longitudinal strain imaging studies of animals with surgically created DVT as the blood clot forms and matures. A well established rat model of DVT was used in this study - this model closely reproduces the development of the clot in clinical disease. Both forward and inverse problems are described in the Theory section of the paper. Specific details of the animal model of DVT, ultrasound strain imaging, and elasticity reconstruction are given in the Materials and Methods section. Results of the elasticity reconstruction are presented in the following section. The paper concludes with a discussion of the results.

2. THEORY

Determining the elastic modulus in an inhomogeneous material from responses to a fixed mechanical action can be formulated using several approaches. These approaches can be generally grouped into two categories: direct and indirect (model-based) reconstruction techniques. If all necessary components of the internal displacement and strain at any point within the object are available, then reconstruction algorithms based on the mechanical equilibrium equations can be used directly to describe the unknown distribution of Young's or shear modulus - these techniques, therefore, belong to direct reconstruction methods. However, if any assumptions about the geometry of the object can be made (i.e., if elasticity variations of the object within the region of interest can be modeled based on the geometry), then a more robust reconstruction can be performed.

For elasticity imaging of DVT, we can assume that the vessel and the blood clot can be modeled such that the elastic modulus within the imaging plane is simply a function of the radial position from an arbitrary origin. This assumption is reasonable and well justified since most blood clots are homogeneous and conform to the somewhat rounded blood vessel. An ultrasound image of a vein with a DVT that extends far beyond the imaging plane is shown in Fig. 1. Clearly, the overall clot can be described as a cylinder within the rounded vessel. In a few cases, where clot is not occlusive or has significant inhomogeneities, this approximation may not be valid and model-based reconstruction will lead to an averaged Young's modulus of the clot. More generally, direct elasticity reconstruction may be required in those cases. However, by assuming a simple model such as this, reconstruction in the vicinity of the vessel and clot is far less susceptible to strain noise than direct reconstruction, i.e., reconstruction based on the complete set of equilibrium equations.

Our model-based elasticity reconstruction technique is based on two successive steps. First, using a mathematical description of DVT, we derive the solution of the forward elastic problem where the displacement and strain fields are determined based on the spatial distribution of Young's modulus in the object and external deformation pattern. Second, the inverse problem is solved iteratively where the solution of the forward problem for a modeled object is compared with experimentally measured strains to estimate the unknown spatial distribution of the Young's modulus. Formulation and solution of both forward and inverse problems are described below.

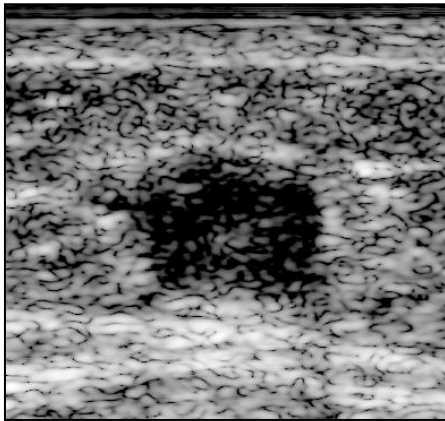


Figure 1. Ultrasound image of the vein with DVT (dark, hypoechoic region in the center). Based on the geometry, the blood clot, vessel and the surrounding tissue can be described using a cylindrically symmetric model where the elastic modulus varies along the radial position from the arbitrary center of origin.

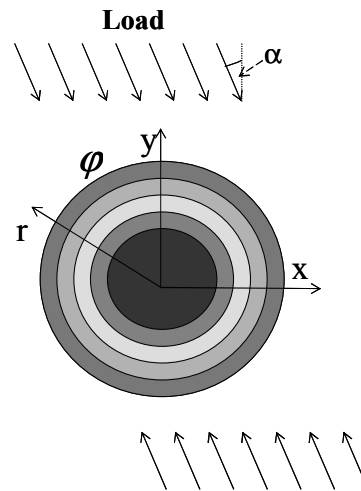


Figure 2. Schematic representation of the DVT deformation model. In this model, the external load is applied at an angle α relative to an ultrasound beam. The blood clot within an occluded vein is approximated as a layered elastic cylinder.

2.1 Forward Problem

Based on the geometry of the blood clot, vessel, and the surrounding tissue (Fig. 1), the forward problem is formulated using a cylindrical coordinate system (r, φ, z) . The clot-containing vessel is modeled as a long cylinder in an infinite medium where the origin of the coordinate system is placed at the center of a cylindrically symmetric vessel and the z -axis is aligned parallel with the vessel's longitudinal axis (Fig. 2).

The elastic modulus distribution across the imaging plane is assumed to be a function of only radial position within the ROI around the clot. A plane strain state¹² is also assumed - this assumption is valid if external loading does not vary, or changes very slowly, along the length of the cylinder such that the gradient of the out-of-plane displacement u_z is either zero or small compared to that of the other two in-plane displacement components (radial u_r and azimuthal u_φ), and the in-plane displacement components do not vary significantly as a function of the out-of-plane coordinate z . The external loading, however, can be applied under some angle α while the ultrasound transducer is still orthogonal to tissue surface, i.e., the ultrasound beams are parallel to the y -axis (Fig. 2).

For a plane strain state, the displacement vector $\vec{U} = (u_r, u_\varphi, 0)$ must satisfy the 2D equations of static equilibrium¹²:

$$\begin{cases} \frac{\partial \sigma_{rr}}{\partial r} + \frac{1}{r} \frac{\partial \sigma_{r\varphi}}{\partial \varphi} + \frac{(\sigma_{rr} - \sigma_{\varphi\varphi})}{r} = 0, \\ \frac{\partial \sigma_{r\varphi}}{\partial r} + \frac{1}{r} \frac{\partial \sigma_{\varphi\varphi}}{\partial \varphi} + 2 \frac{\sigma_{r\varphi}}{r} = 0 \end{cases}, \quad (1)$$

where σ_{rr} , $\sigma_{r\varphi}$, and $\sigma_{\varphi\varphi}$ are components of stress tensor. Here, we consider only incompressible media, because it is well known that soft tissues are very close to incompressible materials¹³. Assuming linear elasticity, the components of the stress tensor in an isotropic, continuous incompressible medium are:

$$\begin{aligned} \sigma_{rr} &= P + 2\mu \varepsilon_{rr}, \quad \sigma_{\varphi\varphi} = P + 2\mu \varepsilon_{\varphi\varphi}, \quad \sigma_{r\varphi} = 2\mu \varepsilon_{r\varphi}, \\ \varepsilon_{rr} &= \frac{\partial u_r}{\partial r}, \quad \varepsilon_{\varphi\varphi} = \frac{1}{r} \frac{\partial u_\varphi}{\partial \varphi} + \frac{u_r}{r}, \quad \varepsilon_{r\varphi} = \frac{1}{2} \left(\frac{1}{r} \frac{\partial u_r}{\partial \varphi} + \frac{\partial u_\varphi}{\partial r} - \frac{u_\varphi}{r} \right), \quad \varepsilon_{zz} = \varepsilon_{rz} = \varepsilon_{\varphi z} = 0, \end{aligned} \quad (2)$$

where μ is a shear elastic modulus, ε_{rr} , $\varepsilon_{\varphi\varphi}$, $\varepsilon_{r\varphi}$, ε_{zz} , ε_{rz} , $\varepsilon_{\varphi z}$, are components of the strain tensor, and P is the static internal pressure. For incompressible media $\mu = E/3$, where E is the Young's modulus, and only one modulus describes the elastic properties of the material. In additional, the incompressibility condition must be satisfied:

$$\text{div} \vec{U} = \varepsilon_{rr} + \varepsilon_{zz} + \varepsilon_{\varphi\varphi} = 0. \quad (3)$$

To satisfy boundary conditions for equations (1-3), the displacements must be zero at $r = 0$, and match the strains applied at infinity.

The solution (1-3) for an arbitrary angle α can be expressed as a combination of uniaxial and shear loads. This solution is presented in detail elsewhere⁹. Briefly, to find the solution of (1-3) for arbitrary $E(r)$ over an ROI, it is assumed that the Young's modulus is constant within each subinterval $[r_i, r_{i+1}]$, i.e., $E(r) = E_i = \text{const}$, $r \in [r_i, r_{i+1}]$, $i = 1 \dots N$, where N is the total number of subintervals covering the region of interest (see Fig. 2). Radial displacement in this interval reduces to:

$$u_r(r, \varphi) = \left(A_i r + B_i r^3 + \frac{C_i}{r} + \frac{D_i}{r^3} \right) \cos(2\varphi), \quad i = 1 \dots N, \quad (4)$$

where arbitrary constants A_i , B_i , C_i , and D_i are different for each ring $[r_i, r_{i+1}]$. These unknown constants can be found using boundary conditions and the stress and displacement continuity conditions at the boundaries of each ring. The expression for azimuthal component of displacement u_φ can be found from incompressibility condition $div\vec{U} = 0$.

2.2 Inverse Problem

In ultrasound strain imaging, the signal-to-noise ratio (SNR) of axial displacement is higher than that of lateral displacements^{14,15}. Therefore, it is desired to construct the inverse problem solution using only one experimentally measured axial component of the strain tensor $\varepsilon_{yy} = \partial u_y / \partial y$, where u_y is axial (i.e., along the ultrasound beam) component of the displacement vector in Cartesian coordinates. Given the Young's moduli over a set of rings, the center of the vessel (x_0, y_0) , the angle α , and the effective deformation at infinity ε_0 applied along this angle, we can compute the theoretical distribution of axial strain. Having experimentally measured the axial strain component $\varepsilon_{yy}^{\text{exp}}$ and using the analytic solution of the forward problem, the unknown Young's modulus E_i can be estimated by minimizing the difference between theoretically predicted and experimentally measured axial strains⁹. In general, the parameters α , ε_0 , and the center (x_0, y_0) of the vein are also unknown and must be estimated simultaneously with the unknown E_i by minimizing the error function. Therefore, the error function takes the form:

$$\delta = \left\| \varepsilon_{yy}^{\text{exp}} - \varepsilon_{yy}^{\text{theory}}(E_i, \varepsilon_0, \alpha, x_0, y_0) \right\|, \quad (5)$$

and elasticity reconstruction reduces to a simultaneous minimization of the error function of (5) with respect to the unknown elasticity distribution, the position of the center of clot, the direction of the effective uniaxial loading of the object, and the magnitude of the effective deformation along this direction.

3. MATERIALS AND METHODS

Animal studies were performed using a rat model of stasis induced venous thrombosis^{8,16-18}. A group of five rats were used in this study although only four animals developed clots. On the first day of the study, all rats underwent surgery to initiate thrombus formation in the inferior vena cava (IVC). As the animals were developing their thrombi progressively from acute/subacute to chronic stage, each rat was imaged on day 3, 4, 5, 6, 7, 8, and 10 using a Siemens "Elegra" ultrasound scanner with a linear 12 MHz array transducer. The transducer was attached to a deformation device to achieve continuous compression on the rat's abdominal wall and underlying tissue. Consecutive frames of ultrasound phase sensitive data were captured in real-time and processed later using a 2D correlation-based phase-sensitive speckle tracking algorithm to derive the strain image of the DVT and surrounding tissue¹⁹.

For each rat, the ROIs for elasticity reconstruction and initial position of the clot center (x_0, y_0) were chosen using the B-scan (Fig. 3a). Each ROI was selected such that it included the IVC and small portion of the surrounding tissue (Fig. 3b) to minimize the elasticity variations of the background tissue. The iteration procedure for elasticity reconstruction consisted two parts. First, for a fixed number of layers, the relative Young's modulus (i.e., Young's modulus of the vessel wall was assigned unity value) was reconstructed by minimizing the error function (5) across the ROI. During each iteration, only one unknown was varied. The iterative parameters which determine step size were chosen taking into account the second order polynomial approximation of δ as a function of each individual E_i under the restriction of decreasing error. If successful, the global linear prediction for all unknowns was used simultaneously after each iteration to reduce oscillation.

Second, to maintain the accuracy of the elasticity reconstruction, the number of rings required to represent the object was iteratively increased until the difference between the current and the previous reconstruction was insignificant. Initially, the reconstruction assumed a homogeneous cylindrical inclusion, i.e., one layer only. With every iteration, the number of layers was increased, and the process was terminated if the relative difference between the current and previous iteration was less than 2%. The number of layers was ranging from 20 to 30 depending on a particular dataset.

4. RESULTS

In strain imaging studies of the rats with DVT, consistent decrease of strain magnitude in the blood clot was observed as DVT develops^{8,18}. These results are consistent with our previous studies⁵⁻⁷ and qualitatively confirm the fact that clot elasticity increases as DVT forms and matures. However, elasticity reconstruction is needed to quantify the clot hardening.

Figure 3 presents an example of the elasticity reconstruction for a rat with 10-day old clot. The overall 10-mm (axial) by 8.5-mm (lateral) B-scan image is shown in Fig. 3a. Using color-flow imaging, the artery adjacent to the IVC was identified while no flow was detected in the IVC signaling that the thrombus had occluded the vessel. On the bottom of the B-scan, the anterior surface of the spine can also be noted. The 4.5-mm by 4.5-mm elasticity reconstruction region (Fig. 3b, also indicated by the white box in Fig. 3a) was chosen to include the entire IVC with the clot located in the center, and a small portion of the background tissue. Once the region of interest was identified, iterative elasticity reconstruction was performed where the experimentally measured axial strain distribution $\epsilon_{yy}^{\text{exp}}$ was compared with the theoretically predicted axial strain map $\epsilon_{yy}^{\text{theory}}$ to minimize the error function (5). The measured normal axial strain image is presented in Fig. 3c over a 0 to 25% strain dynamic range, where full white represents no strain, and full black represents a normal axial strain magnitude of 25% and larger (negative strain indicates that vein size was reduced in vertical direction during the deformation). In this image, the clot has lower strain magnitude compared to the vessel wall immediately surrounding the clot. The resultant Young's modulus distribution E_i over a set of rings is presented in Fig. 3d where a gray-scale map is used to display the relative Young's modulus over the 0.7 to 1.0 range. The gray-scale map was selected so that full black corresponds to a relative Young's modulus of less than or equal to 0.7, while white areas represent harder tissue. Clearly, the clot overall appears to be harder and, therefore, has higher Young's modulus compared to the outer regions. Finally, Fig. 3e presents the theoretically predicted axial strain distribution corresponding to reconstructed values of Young's modulus in Fig. 3c.

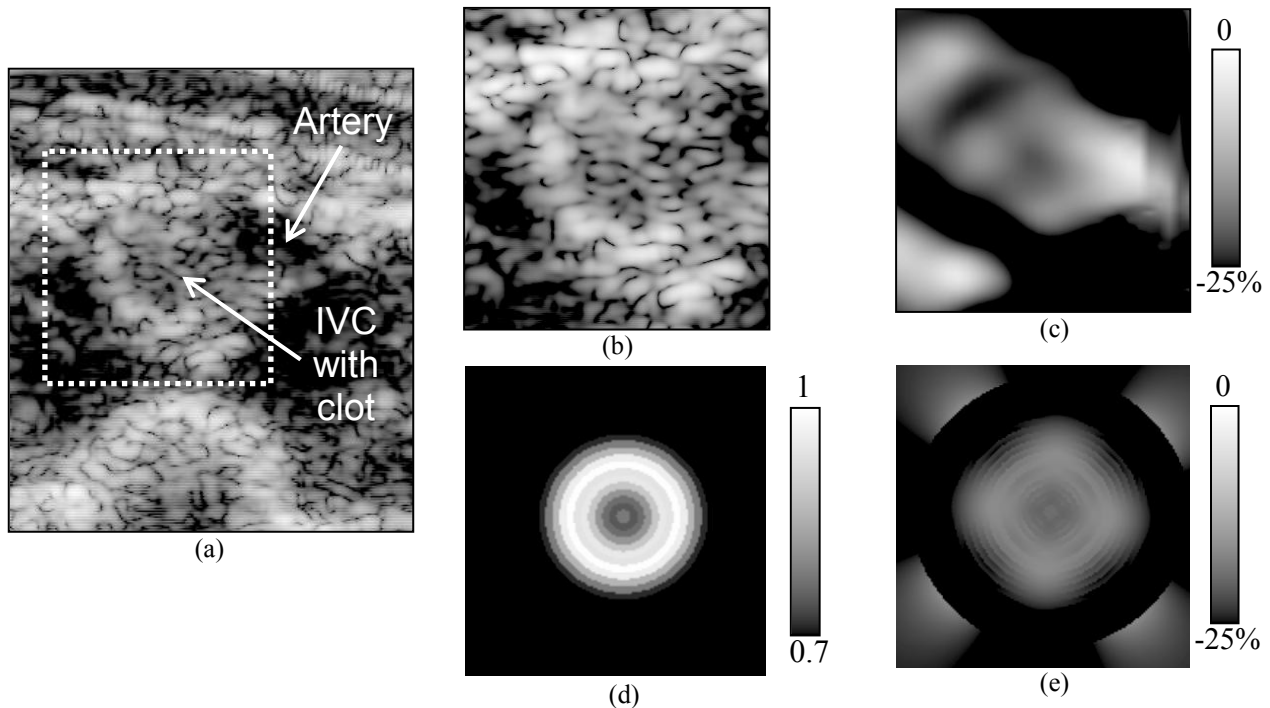


Figure 3. Elasticity reconstruction procedure demonstrated for a rat with a 10-day old clot. a) Overall B-scan image of rat's abdomen. b) Elasticity reconstruction region. c) Measured axial strain within ROI. d) Young's modulus reconstruction, and e) corresponding theoretical strain image.

Further analysis of clot elasticity is presented in Fig. 4 where the Young's modulus profile along the center of the clot is plotted. The clot itself has some variation of elasticity but overall remains harder than the background tissue. In fact, on average the clot is even harder than the vessel wall. Figure 5 depicts quantitative comparison of experimental and theoretical strain profiles along the center vertical line of images in Figs. 3c and 3e. Good agreement between measurement and theory is demonstrated even for the complex in-vivo environment and boundary conditions encountered in these studies.

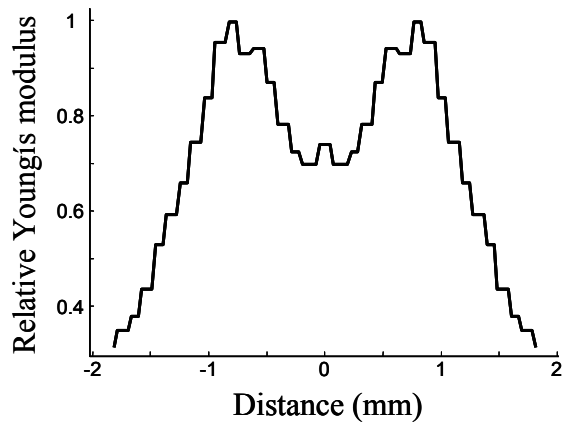


Figure 4. The central profile through the reconstructed elasticity image

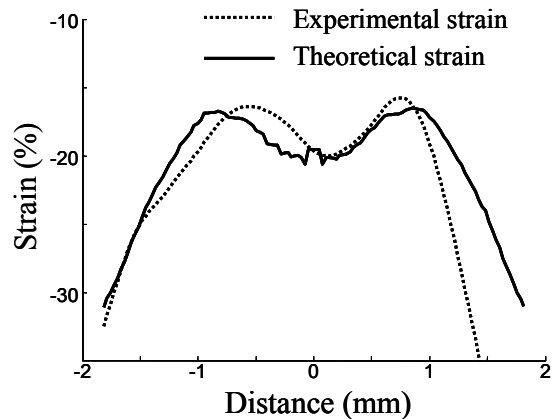


Figure 5. The central profiles through experimental and theoretical strain images.

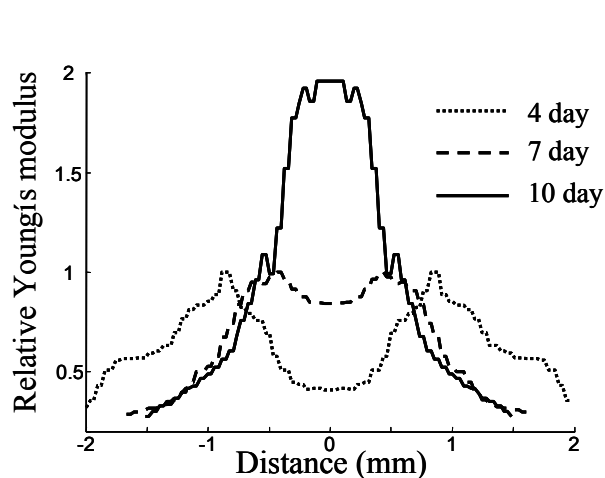


Figure 6. Young's modulus profiles for 4- (acute), 7- (subacute) and 10-day old (chronic) clots.

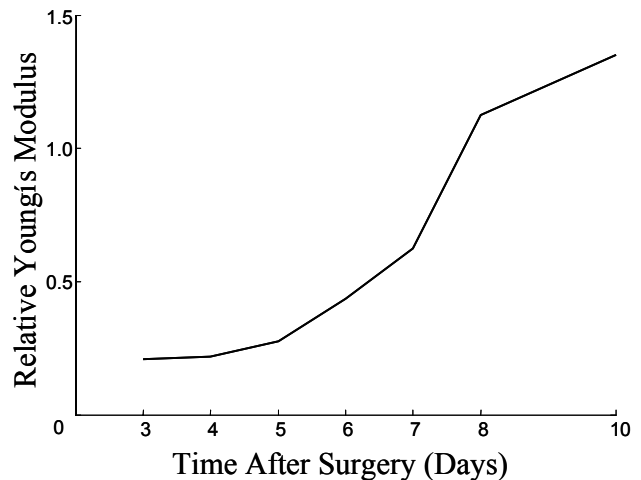


Figure 7. Changes in the Young's modulus of the clot during formation and aging of DVT.

Figure 6 contrasts relative Young's modulus of the clot in another animal at 4, 7 and 10 days after the surgery. In this animal model of DVT, 3- to 4-day old clot represents an acute clot, 6- to 7-day old clot represents a subacute DVT, and 10-day old clot represents a chronic clot. The rate of clot growth is different in humans, but the process of clot formation has the same stages. As blood clot develops, clot elasticity is increasing from about 0.25 to 2.0 relative to the vessel wall. This is further illustrated in Fig. 7, where relative Young's modulus is plotted as function of time after surgery, i.e., age of the clot. In Figure 7, the elasticity values were averaged for four rats that were used in our study. Clearly, the relative elasticity of the clot is increasing with clot age suggesting that Young's modulus can be used to age DVT.

5. DISCUSSION AND CONCLUSIONS

The results of elasticity reconstruction confirm the hypothesis that blood clot hardens as it matures. Indeed, the Young's modulus of thrombi increases over time, and 10-day old clot is approximately 3-6 times higher than that of the 3-day old clot. For each animal, however, the elasticity of clots is increasing, but not always monotonically. This fact can be explained by several sources of errors in strain measurements and reconstruction. For example, in our longitudinal studies, each animal is scanned once every 24 hours, but the imaging plane is not necessarily the same from one scan to the next. Another source of elasticity reconstruction errors could lie in the selection of the ROI. For example, part of the artery was also included into the rectangular ROI (Fig. 3b). Such inclusion, however, is not generally desired due to strain imaging artifacts often associated with the aortic region. This is because of the high (approximately 200 Hz) heart rate of the small animals, and insufficient temporal sampling of this region using conventional ultrasound imaging. Generally, this will not represent a problem in clinical settings, and could be even eliminated in animal studies if the region of interest can be made arbitrarily. Nevertheless, the elasticity variations are not significant and overall do not jeopardize the ability of elasticity imaging to age DVT.

The elasticity reconstruction approach produces maps of relative Young's modulus. For all results presented in this paper, the Young's modulus was normalized to wall of the vessel, i.e., it was assumed that the elasticity of the vessel wall does not change. This, in fact, may not be a valid assumption as the body responds to the disease. For example, the vessel wall undergoes inflammation that could increase tissue elasticity. This, however, will only further enhance the contrast in absolute Young's modulus. Therefore, absolute elasticity reconstruction may provide an even better mechanism for DVT aging. Our model is capable of absolute elasticity reconstruction if the load (or surface stress at one point) can be measured. We are currently performing studies to investigate this issue.

In conclusion, results of our studies indicate that Young's modulus gradually increases with clot formation and, therefore, ultrasound elasticity imaging can age deep venous thrombosis. Hence, today's "gold standard" for DVT detection - conventional venous duplex ultrasound imaging - could incorporate elasticity imaging to become a clinical tool for thrombosis detection, diagnosis and staging.

ACKNOWLEDGMENTS

Supported in part by National Institutes of Health under grants DK47324, HL47401, HL67647, CA69568, and HL68658, U.S. Army Medical Research and Materiel Command under grants DAMD17-02-1-0097 and DAMD17-01-1-0562, and the Ultrasound group of Siemens Medical Systems, Inc. (Issaquah, WA) is gratefully acknowledged.

REFERENCES

1. J. Hirsh, and J. Hoak, "Management of deep vein thrombosis and pulmonary embolism. A statement for healthcare professionals. Council on Thrombosis (in consultation with the Council on Cardiovascular Radiology)," *American Heart Association. Circulation*, vol. 93(12), pp 2212-2245, 1996.
2. T.M. Hyers, G. Agnelli, R.D. Hull, J.G. Weg, T.A. Morris, M. Samama and V. Tapson, "Antithrombotic therapy for venous thromboembolic disease," *Chest*, 114 (Supplement 5), pp 561S-578S, 1998.
3. R.D. Hull, G.E. Raskob, D. Rosenbloom, A.A. Panju, P. Brill-Edwards, J.S. Ginsberg, J. Hirsh, G.J. Martin, D. Green, "Heparin for 5 days as compared with 10 days in the initial treatment of proximal venous thrombosis," *N. Engl. J. Med.*, 322, pp 1250-1264, 1990.
4. B.D. Lewis. "The peripheral veins" In: C.M. Rumack, S.R. Wilson, J.W. Charboneau (eds), *Diagnostic Ultrasound*, 2nd Edition, Mosby, St. Louis, MO, pp 946-954, 1998.
5. S.Y. Emelianov, J.M. Rubin, X. Chen, A.R. Skovoroda, T.W. Wakefield and M. O'Donnell, "Ultrasound elasticity imaging of deep venous thrombosis," in Proc. of *IEEE Ultrasonics Symp.*, pp 1791-1794, 2000.
6. S.Y. Emelianov, X. Chen, M. O'Donnell, B. Knipp, D. Myers, T.W. Wakefield, and J.M. Rubin, "Triplex ultrasound: Elasticity imaging to age deep venous thrombosis," *Ultrasound Med. Biol.*, vol. 28, pp 757-767, 2002.

7. J.M. Rubin, S.R. Aglyamov, T.W. Wakefield, M. O'Donnell, S.Y. Emelianov, "Clinical application of sonographic elasticity imaging for aging of deep venous thrombosis: preliminary findings," *J Ultrasound Medicine* 22 (5): 443-448, 2003.
8. H. Xie, J. M. Rubin, K. Kim, W. F. Weitzel, X. Chen, S.R. Aglyamov, S.Y. Emelianov, M. O'Donnell, S. K. Wroblewski, D. D. Myers and T. W. Wakefield, "Elasticity imaging to stage deep vein thrombosis treatment," *Ultrasonic Imaging*, 25, pp 52-53, 2003.
9. S.R. Aglyamov, A.R. Skovoroda, J.M. Rubin, M. O'Donnell and S.Y. Emelianov, "Model-based reconstructive elasticity imaging of deep venous thrombosis," *IEEE Trans. Ultrason., Ferroelect., and Freq. Contr.*, in press, 2004.
10. A.R. Skovoroda, S.Y. Emelianov, M.A. Lubinski, A.P. Sarvazyan and M. O'Donnell, "Theoretical analysis and verification of ultrasound displacement and strain imaging", *IEEE Trans. Ultrason., Ferroelect., and Freq. Contr.*, vol. 41, pp 302-313, 1994.
11. K.J. Parker, L. Gao, R.M. Lerner and S.F. Levinson, "Techniques for elastic imaging: a review," *IEEE Engin. Med. Biol. Magazine*, vol. 15(6), pp 52-59, 1996.
12. S. Timoshenko and J. Goodier, "*Theory of elasticity*," New-York: McGraw-Hill, 1951.
13. A.P. Sarvazyan, "Low frequency acoustic characteristics of biological tissues," *Mech. Polymers*, vol. 4, pp 691-695, 1975.
14. M.A. Lubinski, S.Y. Emelianov, K.R. Raghavan, A.E. Yagle, A.R. Skovoroda and M. O'Donnell, "Lateral displacement estimation using tissue incompressibility," *IEEE Trans. Ultrason., Ferroelect., and Freq. Contr.*, vol. 43, pp 247-255, 1996.
15. E.E. Konofagou and J. Ophir, "A new method for estimation and imaging of lateral strains and Poisson's ratios in tissues," *Ultrasound Med. Biol.*, vol. 24(8), pp 1183-1199, 1998.
16. D.D. Myers, S.K. Wroblewski, P.K. Henke, T.W. Wakefield, "Coagulation biology," in: W. Souba, D. Wilmore (eds): "*Surgical Research*," Academic Press, San Diego, CA, pp 989-1000, 2001.
17. T.W. Wakefield, R.M. Strieter, C.A. Wilke, A.M. Kadell, S.K. Wroblewski, M.D. Burdick, R. Schmidt, S.L. Kunkel, L.J. Greenfield, "Venous thrombosis-associated inflammation and attenuation with neutralizing antibodies to cytokines and adhesion molecules," *Arterioscler. Thromb. Vasc. Biol.*, vol. 15, pp 258-268, 1995.
18. H. Xie, K. Kim, S.R. Aglyamov, S.Y. Emelianov, X. Chen, M. O'Donnell, W. F. Weitzel, S.K. Wroblewski, D.D. Myers, T.W. Wakefield and J.M. Rubin "Demonstration of staging deep venous thrombosis using ultrasound elasticity imaging: animal model," submitted for publication in *Ultrasound Med. Biol.*, 2004.
19. M.A. Lubinski, S.Y. Emelianov and M. O'Donnell, "Speckle tracking methods for ultrasonic elasticity imaging using short-time correlation," *IEEE Trans. Ultrason., Ferroelect., and Freq. Contr.*, vol. 46, pp 82-96, 1999.